sciendo

Polish Journal of Chemical Technology, 22, 3, 24—28, 10.2478/pjct-2020-0024

Nitrogen-doped Carbon Catalyst by Ultrasonic for Electrocatalytic CO_2 Reduction

Jianfeng Liu[1, 2], Ting Wang[1], Zhenhai Zhang[1], Kai Ning[1], Shibin Yin[2], Binxia Yuan[1, 2*]

1. College of Energy and Mechanical Engineering, Shanghai University of Electric Power, Shanghai, 200090, China
2. Key Laboratory of New Processing Technology for Non-ferrous Metals and Materials (Ministry of Education), Guangxi Key Laboratory of Processing for Non-ferrous Metals and Featured Materials, Nanning Guangxi 530004, China
[*]Corresponding authors: e-mail: : janice.liujianfeng@gmail.com; yuanbinxia100@163.com

The electrocatalytic reduction of carbon dioxide into valued chemicals such as formic acid has the most promising potential in applying renewable energy for useful materials and mitigating the greenhouse effect. However, the studies still focus on developing catalysts with low price and high catalytic properties. In this study, nitrogen atoms were decorated into carbon structure by a unique ultrasonic method, then the nitrogen-doped carbon material was applied as catalyst in CO_2 reduction, it exhibited excellent electrochemical activity, 4 times higher than the normal method. The improved activity should be attributed to the interaction between nitrogen and carbon atoms through analysis.

Keywords: Nitrogen-doped; Catalyst; Ultrasonic; CO_2 Reduction.

INTRODUCTION

The carbon dioxide emission already causes a global serious issue due to the irreversible effects on world's climate and human survival[1–4]. CO_2 re-utilization via electrochemical method is one of the most attractive approaches for generating active product. It also reduces the affect of greenhouse, receives energy-dense substances and accomplishes the great cycle of carbon[5–11]. Carbon material was widely reported in CO_2 reduction owing to its lower price and higher stability than precious metals such as platinum, palladium, gold, silver and so on[12–14]. There are also other normal metal materials applied for CO_2 reduction. Mou et al.[15] displayed a boron phosphide nanoparticles with a high Faladaic efficiency of 92%. Sun et al.[16–17] prepared a 2D $Fe_2P_2S_6$ nanosheet and an FeP nanoarray with the Faladaic efficiency of 88% and 94%, respectively. Obviously, Ketjen black carbon (KB) is considered as a promising carbon due to its unique chainlike structure, excellent electrochemical stability, high conductivity, large surface area and low price.[18] Impressive studies have been carried out to improve the catalytic activity by thermal treatment or incorporating KB with other elements. Miyake demonstrated that KB modified by acid, glucose dehydrogenase and oxidized nicotinamide adenine dinucleotide obtained impressive oxidization of glucose with tiny voltage and maximum power density of 52 μW cm^{-2} in biofuel cells[19]. Nabae group reported that KB showed excellent catalytic activity with over 90% yield over 50°C and high stability under aerobic oxidations of hydrocarbons[20]. Tashima et al. showed that KB material prepared by vacuum pre-treatment and thermal treatment in argon performed high energy density and 181 F g^{-1} anode capacitance which was superior to untreated in supercapacitors[21]. Li and his co-workers discovered a novel boron-doped KB catalyst which exhibited extremely high discharge capacity of 7193 mA h g^{-1} and long cycle life in non-aqueous rechargeable Li-O_2 batteries[22]. Nevertheless, decorating or treatments with KB to promote catalytic properties still attracts researchers' attention.

Nitrogen atom is similar to carbon, and show strong interactions with carbon atoms. The nitrogen-doped carbon materials have been increasingly studied in electrochemical and photo-electrochemical fields as active materials[23–25]. Wu et al. discovered that nitrogen-doped carbon nanotubes with total N content of 5 at% received over-potential of –0.18 V and stable catalytic properties of electrochemical CO_2 reduction[26]. Zhang et al.[27] reported that a 3D nitrogen-doped carbon nanomaterial exhibited maximum Faradaic efficiencies of 87% with current density of 9.5 mA cm^{-2}. Recently, Xu et al.[28] showed that a N-doped carbon nanotube towards electrocatalytic reduction of CO_2 with current efficiency of 90%. Bi group[29] reported that three dimensional nitrogen-doped porous carbons synthesized by one-step pyrolysis of solid mixture of sodium citrate and melamine exhibited maximum power density of 2777.7 Mw m^{-2}, approximately twice higher than commercial carbon in microbial fuel cells. Despite these researches, the type of chemical bond and distribution of nitrogen element on carbon materials, which could foster high catalytic properties, has yet not been controlled successfully. In this study, we decorate nitrogen atoms into KB structure via a unique ultrasonic method, and then apply the material as electro-catalyst for electrocatalytic reduction of carbon dioxide.

EXPERIMENT

Materials

Chemicals are analytic reagent grade and use as received without further purification. Isopropanol, alcohol, 5 wt% Nafion dispersion solution and potassium hydrogen carbonate are purchased from Wako. Urea is obtained from Sinopharm Chemicals. Ketjen black EC-600JD (KB) used as carbon material is supplied by Lion. Deionized water is used in all cases.

Electrocatalyst synthesis

The typical preparation process of the N-doped KB catalyst is schematically described in Figure 1. Specifically, a moderate amount of Ketjen black is heated at 1200°C for 2 h with the heating rate of 10°C min^{-1} in N_2 (80 mL min^{-1}), and cool down to room temperature

naturally, then marked as KB1200. 100 mg KB1200 powder and 300 mg urea are mixed with 0.5 ml alcohol, then the mixture is put into ultrasonic bath for 100 min with ice bath and room temperature water respectively. The product is dried at 60°C overnight. The second pyrolysis step is performed in a tube furnace at 900°C for 2 h (N_2, 80 ml min^{-1}, 10°C min^{-1}). The black powder is removed from furnace after cooling down to room temperature naturally. The received samples are labeled as NKB-U-ICE and NKB-U. For contrast, another sample is synthesis with similar process without ultrasonic treatment, marked as NKB.

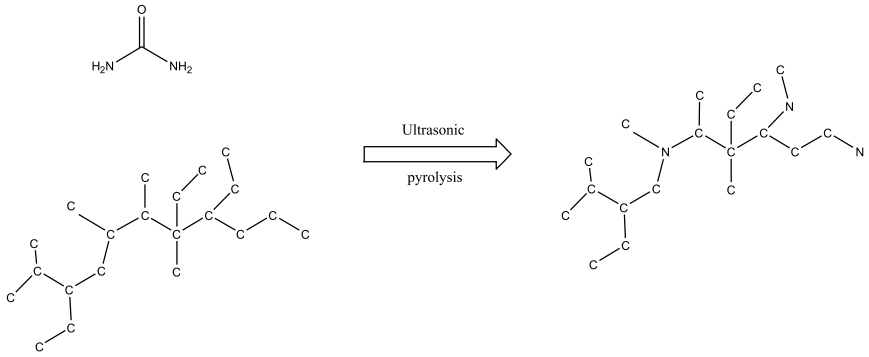

Figure 1. Schematic illustration of formation procedure of N-doped KB catalyst

Characterizations

Materials are characterized by the scanning electron microscope (SEM, JSM-7800F) for morphology and microstructure. The specific surface area (BET) is reported by N_2 adsorption at 77 K using testing systems (Quantachrome autosorb iQ). X-ray diffraction (XRD, D8 DaVinci) is performed at a scanning rate of 10° min^{-1} at the diffraction angle ranging from 10 to 90°. The Raman spectroscopy is recorded using a test instrument (Raman, Labram HR Evolution) with an excitation wavelength of 633 nm. Moreover, the X-ray photoelectron spectroscopy (XPS, AXIS ULTRA DLD) is used to verify the surface compositions and element states.

Working Electrode Preparation

All labeled samples are dispersed in a mixture of deionized water, isopropanol and 5 wt% Nafion dispersion solution in a volume ratio of 1:1:0.01. The catalyst solution is dispersed by ultrasonic for 30 min in ice bath. Then, a smooth glassy carbon-disk electrode (0.196 cm^2, Hokuto Denko) is carefully covered with the catalytic ink and dry at 60°C for 10 min. Finally, the loading on working electrode is 9.7 μg cm^{-2}.

Electrochemical Measurements

Electrochemical measurements are performed by a typical rotating disking electrode system (HZ-7000, HOKUTO DENKO) in CO_2-saturated 0.5 M $KHCO_3$ electrolyte. The three-electrode system is employed to characterize the catalytic properties. The glassy carbon disk electrode coating with catalysts is used as working electrode. An Ag/AgCl electrode filled with saturated KCl solution works as reference electrode, a platinum electrode works as the counter electrode. The linear sweep voltammograms (LSV) are recorded from 0 V to –2 V vs. $_{Ag/AgCl}$ in CO_2 saturated 0.5 M $KHCO_3$ with a scan rate of 10 mV s^{-1} at 400, 900, 1600 and 2500 rpm respectively.

RESULTS AND DISCUSSION

The morphology of these carbon materials by SEM is shown in Figure 2. It is obviously observed that commercial KB performs a highly stacked three-dimensional structure with disordered branches and rough surface. This indicates that commercial KB has highly porosity. After heat treatment, KB1200, NKB-U and NKB-U--ICE show similar microstructure to commercial KB, it reveals that heat treatment and N doping lead to no obvious difference in morphology. It maybe because the treatment temperature is only 1200°C which is not enough to cause significant change in this carbon structure. According to calculation by the N_2 adsorption method, Brunauer-Emmett-Teller surface area and pore size, are 1351.702 m^2 g^{-1} and 3.825 nm for KB compared with 1454.378 m^2 g^{-1} and 3.83 nm for KB1200, consistent with the results from SEM images.

The powder XRD pattern for the five samples shown in Figure 3. It can be seen the typical broad peaks at 22° and 43° for KB1200, they are well indexed to (002) and (100) planes of carbon. All the nitrogen doped KB samples display a peak at 26°, which also corresponds to (002) crystal plane. But in this case, the broad peak suggests the defective nature of the nitrogen-doped materials. Compared with KB1200, N-doped KB performs small and broad peaks, which indicates the low crystallization caused by N-doping. Obviously, for the catalyst prepared at ice bath (NKB-U-ICE), fairly small and broad peaks are obtained, demonstrating that the more nitrogen atoms are decorated in KB affecting the catalytic activities eventually.

To further investigate the phases of catalysts, Raman spectrum is shown in Figure 4. The two peaks at 1340 cm^{-1} and 1597 cm^{-1} for KB are observed, correspond to D band and G band. The D peak and G peak are at the same position for all the KB samples. The D peak for NKB-U-ICEis broader than other N-doped samples, and the intensity ratio of the D and G peaks (I_D / I_G = 1.25) of NKB-U-ICE is larger than that of NKB-U (I_D / I_G = 1.23), NKB (I_D / I_G = 1.24). That means NKB-U-ICE sample shoes more disorder structure.

Figure 5 shows the XPS spectrum for KB samples. A strong C 1s signal for carbon at 285 eV is observed, with O 1s for oxygen at 530 eV, and N 1s for nitrogen at 400 eV. There is 1.37 at% nitrogen in NKB-U-ICE,

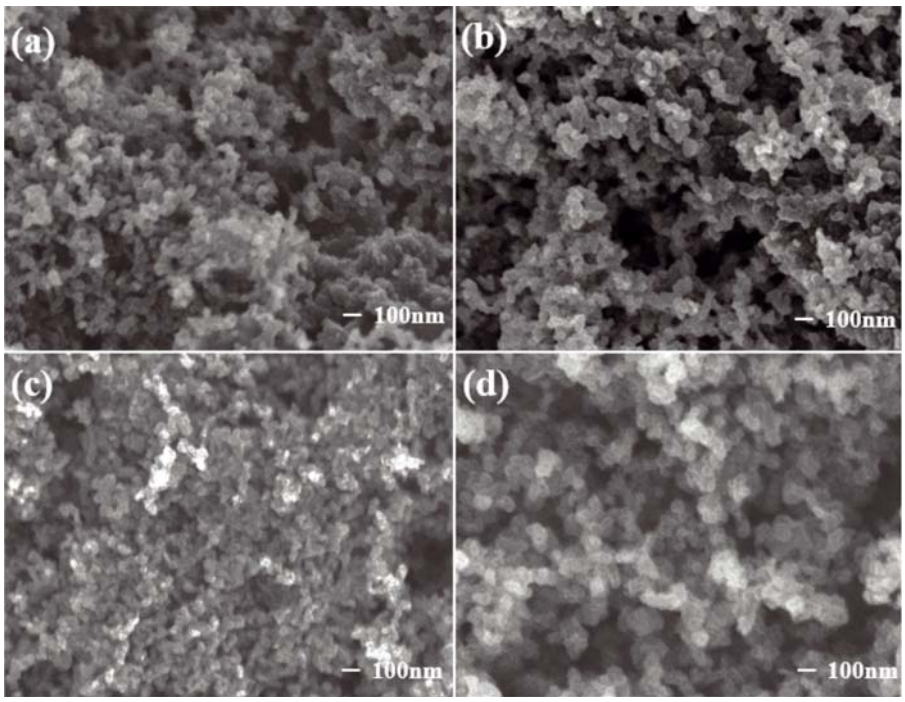

Figure 2. SEM images of (a) KB; (b) KB1200; (c) NKB-U; (d) NKB-U-ICE

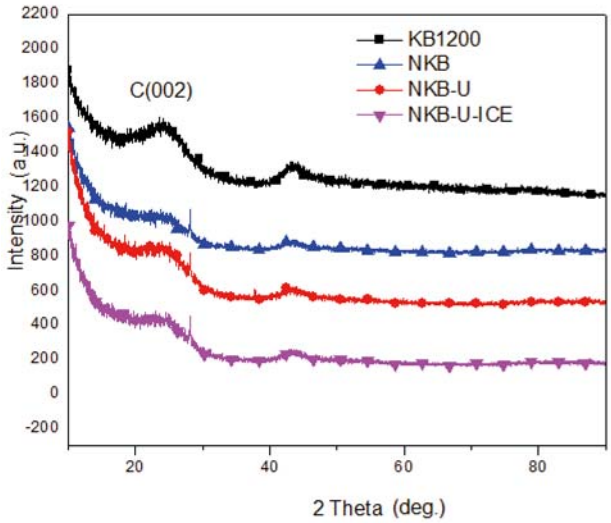

Figure 3. XRD patterns of KB1200, NKB, NKB-U and NKB--U-ICE

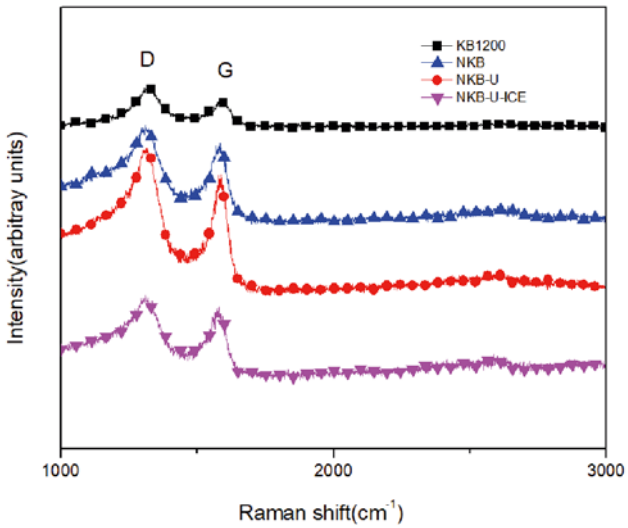

Figure 4. Raman spectra of KB1200, NKB, NKB-U and NKB--U-ICE

compared with 0.66 at% for NKB-U, 0.72 at% for NKB. The N content in NKB is similar to NKB-U, that means ultrasonic in water bath during the synthesis process (NKB-U) is not different to none ultrasonic sample (NKB). However, when the water bath is changed to ice bath in ultrasonic process, the N content is increase 2 times. Therefore, it can be thought that ultrasonic in ice bath can affect the nitrogen doping amount. This is maybe duo to the low temperature in ultrasonic process, which can prevent urea evaporation during ultrasonic in ice bath. The relatively large oxygen signal may be due to the moisture in samples. Figure 5b–d show the N1s spectrum for nitrogen element. These N1s peaks include three main components, related to pyridinic nitrogen (398.3 eV) that is dominant all the time for active sites, pyrrolic nitrogen (400 eV) and graphitic nitrogen (401.3 eV) as well as a small shoulder at about 397 eV, which may correspond to dehydrogenized pyrrole or imine groups. Comparing the N 1s peak of samples, the percent of pyridinic nitrogen in total nitrogen content increase, which consistent with the trend of nitrogen content.

The electrochemical activity measurements for KB, KB1200, NKB, NKB-U and NKB-U-ICE were performed to evaluate the activity of catalysts in CO_2 saturated 0.5 M $KHCO_3$ electrolytes, using a rotating disk electrode (RDE) system. The Linear sweep voltammetry (LSV) curves for KB samples are shown in Figure 6. In the insert graph of Figure 6, the onset potential V_{onset} is defined as the voltage at –0.05 mA cm^{-2}. For sample NKB-U-ICE, the onset potential is –1.41 $V_{Ag/AgCl}$, 20 mV higher than NKB (–1.43 $V_{Ag/AgCl}$), but 20 mV lower than NKB-U (–1.39 $V_{Ag/AgCl}$), 50mV lower than KB (–1.36 $V_{Ag/AgCl}$) and 60 mV lower than KB1200 (–1.36 $V_{Ag/AgCl}$). NKB-U-ICE shows a relatively low onset potential. It is observed that N-doped KB samples perform high mass transport limitation current as –8.0 mA/cm^2 in NKB--U-ICE, compare with –4.0 mA/cm^2 in NKB, –3.7 mA/cm^2 in NKB-U, –2.4 mA/cm^2 in KB1200 and –1.9 mA/cm^2 in KB respectively. Obviously, NKB-U-ICE shows

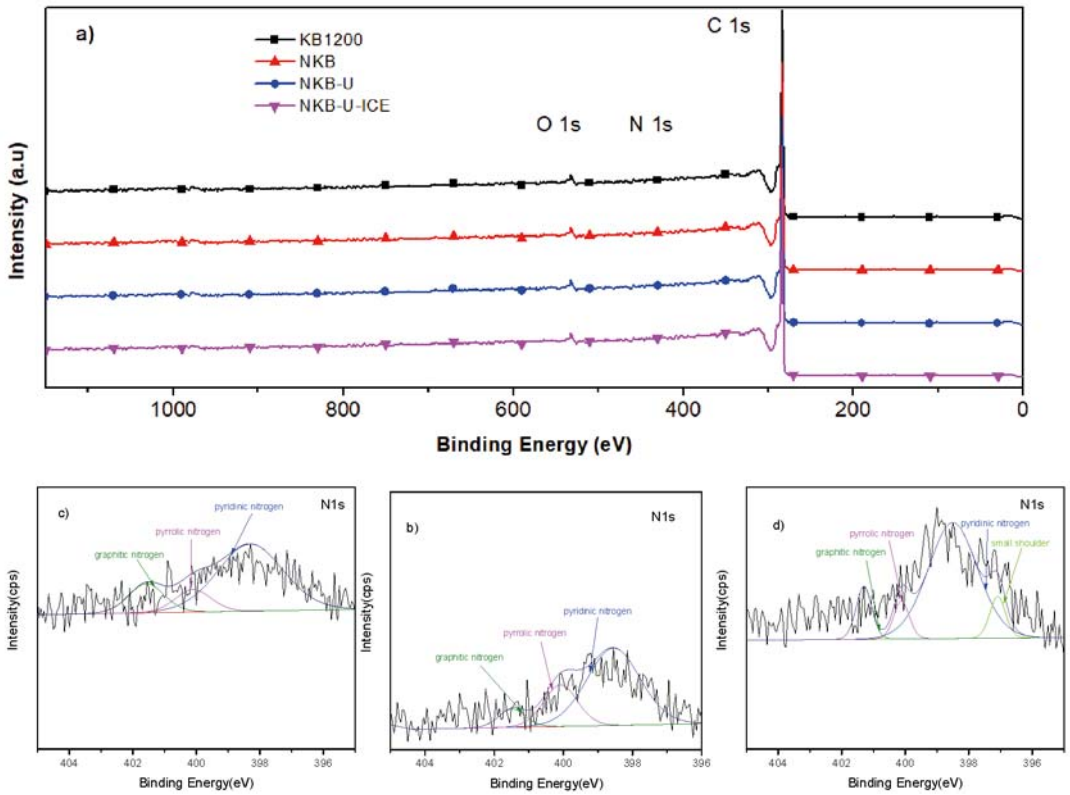

Figure 5. (a) XPS survey spectra of KB1200, NKB, NKB-U and NKB-U-ICE. (b) N1s region of NKB-U. (c) N1s region of NKB. (d) N1s region of NKB-U-ICE

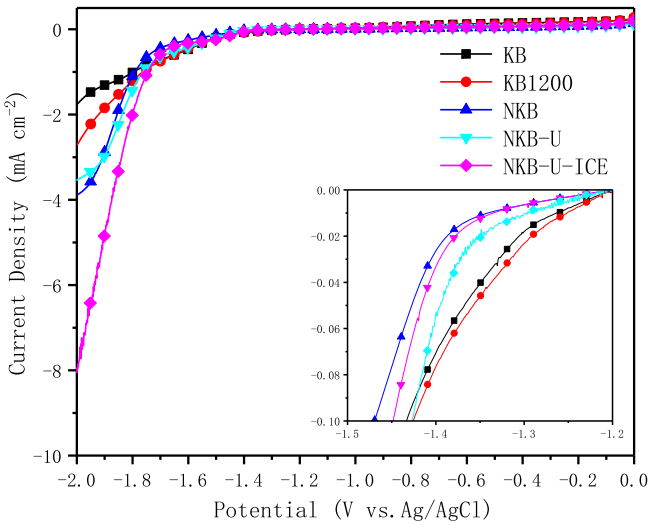

Figure 6. LSV disk currents of KB, KB1200, NKB, NKB-U and NKB-U-ICE

excellent performance in LSV disk current, but it still very low than other study with noble metal catalysts.

Finally, catalyst NKB-U-ICE show the optimal catalytic activity as indicated by the highest current density. The excellent activity of NKB-U-ICE is owed to the nitrogen content and the interaction between carbon and nitrogen. That is to say, the activity of catalysts maybe attribute to the increase of pyridinic nitrogen, which is active sites for oxygen reduction reaction.

CONCLUSIONS

We prepared nitrogen-doped KB carbon by a simple, special ultrasonic method. The specific surface area was >1000 m^2 g^{-1}, nitrogen content is 1.37 at%. When applied as oxygen reduction reaction catalyst in carbon dioxide reduction, this material showed good activity, higher than the other related materials. Linear sweep voltammetry revealed an onset potential of –1.34 $V_{Ag/AgCl}$, a mass transport limitation current of –8.0 mA $^{cm-2}$. The special ultrasonic process may supply more sites for the reaction between nitrogen and carbon atoms in the next pyrolysis, and affect the interaction between carbon and nitrogen atoms to form more pyridinic nitrogen. This result is consistent with other's study. The special ultrasonic method can increase catalytic activity for KB carbon material. However, further work needs to be done to increase the catalyst capacity for carbon dioxide reduction before the commercial apply.

ACKNOWLEDGMENT

This work was supported by the financial supports from Open Foundation of Guangxi Key Laboratory of Processing for Non-ferrous Metal and Featured Materials (Grant No. 2020GXYSOF17)

LITERATURE CITED

1. Nabipour, N. & Iranshahi, D. (2017). Novel Chemical Looping Combustion Assisted Residue Fluid Catalytic Cracking Process in Order To Reduce CO_2 Emission and Gasoline Production Enhancement. *Energy & Fuels* 31 (5), 5662–5672. DOI: 10.1021/acs.energyfuels.7b00169.

2. Oschatz, M. & Antonietti, M. (2018). A search for selectivity to enable CO_2 capture with porous adsorbents. *Energy & Environ. Sci.* 11 (1), 57–70. DOI: 10.1039/C7EE02110K.

3. Li, X., Anderson, P., Jhong, H., Paster, M., Stubbins, J. &Kenis, P. (2016). Greenhouse Gas Emissions, Energy Efficiency, and Cost of Synthetic Fuel Production Using Electrochemical

CO_2 Conversion and the Fischer–Tropsch Process. *Energy & Fuels* 30 (7), 5980–5989. DOI: 10.1021/acs.energyfuels.6b00665.

4. Zhao, S., Ma, L., Yang, J., Zheng, D., Liu, H. & Yang, J. (2017). Mechanism of CO_2 Capture Technology Based on the Phosphogypsum Reduction Thermal Decomposition Process. *Energy & Fuels* 31 (9), 9824–9832. DOI: 10.1021/ acs.energyfuels.7b01673.

5. Gong, J., Zhang, L. & Zhao, Z. (2017). Nanostructured Materials for Heterogeneous Electrocatalytic CO_2 Reduction and Related Reaction Mechanisms. Angewandte Chemie International Edition. DOI: 10.1002/anie.201612214.

6. Kornienko, N., Zhao, Y., Kley, C.S., Zhu, C., Kim, D., Lin, S., Chang, C.J., Yaghi, O.M. & Yang, P. (2015). Metal--organic frameworks for electrocatalytic reduction of carbon dioxide. *J. Am. Chem. Soc.* 137 (44), 14129–35. DOI: 10.1021/ jacs.5b08212

7. Vasileff, A., Yao, Z. & Shi, Z. (2017). Carbon Solving Carbon's Problems: Recent Progress of Nanostructured Carbon--Based Catalysts for the Electrochemical Reduction of CO_2. *Adv. Energy Mater.* 7 (21), 1700759. DOI: 10.1002/aenm.201700759

8. Gutiérrez-Guerra, N., Moreno-López, L., Serrano-Ruiz, J., Valverde, J. & de Lucas-Consuegra, A. (2016). Gas phase electrocatalytic conversion of CO_2 to syn-fuels on Cu based catalysts-electrodes. *Appl. Catal. B: Environ*. 188, 272–282. DOI: 10.1016/j.apcatb.2016.02.010.

9. Gao, S., Lin, Y., Jiao, X., Sun, Y., Luo, Q., Zhang, W., Li, D., Yang, J. & Xie, Y. (2016). Partially oxidized atomic cobalt layers for carbon dioxide electroreduction to liquid fuel. *Nature* 529 (7584), 68. DOI: 10.1038/nature16455.

10. Lin, S., Diercks, C., Zhang, Y., Kornienko, N., Nichols, E., Zhao, Y., Paris, A., Kim, D., Yang, P., Yaghi, O. & Chang, C. (2015). Covalent organic frameworks comprising cobalt porphyrins for catalytic CO_2 reduction in water. *Science* 349 (6253), 1208–1213. DOI: 10.1126/science.aac8343.

11. Gao, D., Zhou, H., Wang, J., Miao, S., Yang, F., Wang, G., Wang, J. & Bao, X. (2015). Size-Dependent Electrocatalytic Reduction of CO_2 over Pd Nanoparticles. *J. Amer. Chem. Soc.* 137 (13), 4288. DOI: 10.1021/jacs.5b00046.

12. Tao, L., Wang, Q., Dou, S., Ma, Z., Huo, J., Wang, S. & Dai, L. (2016). Edge-rich and dopant-free graphene as a highly efficient metal-free electrocatalyst for the oxygen reduction reaction. *Chem. Commun.* 52 (13), 2764–2767. DOI: 10.1039/ c5cc09173j.

13. Xu, L., Jiang, Q., Xiao, Z., Li, X., Huo, J., Wang, S. & Dai, L. (2016). Plasma-Engraved Co_3O_4 Nanosheets with Oxygen Vacancies and High Surface Area for the Oxygen Evolution Reaction. *Angew. Chem. Internat. Edit.* 55 (17), 5277–5281. DOI: 10.1002/ange.201600687.

14. Li, R., Hu, D., Zhang, S., Zhang, G., Wang, J. & Zhong, Q. (2015). Spinel Manganese–Cobalt Oxide on Carbon Nanotubes as Highly Efficient Catalysts for the Oxygen Reduction Reaction. Energy Technol. 3 (12), 1183–1189. DOI: 10.1002/ ente.201500156.

15. Mou, S., Wu, T., Xie, J., Zhang, Y., Ji, L. & Huang, H. (2019). Boron phosphide nanoparticles: a nonmetal catalyst for high-selectivity electrochemical reduction of CO_2 to CH_3OH. *Adv. Mater*. 31(36), 1903499.1–6. DOI: 10.1002/ adma. 201903499.

16. Ji, L., Chang, L., Zhang, Y., Mou, S. & Sun, X. (2019). Electrocatalytic CO_2 reduction to alcohols with high selectivity over two-dimensional $Fe_2P_2S_6$ nanosheet. ACS Catal., 2019(XXXX). DOI: 10.1021/acscatal.9b03180.

17. Ji, L., Li, L., Ji, X., Zhang, Y., Mou, S. & Wu, T. (2020). Highly selective electrochemical reduction of co2 to alcohols on an fep nanoarray. *Angew. Chemie Internat. Edit.* 59(2). DOI: 10.1002/ange.201912836.

18. Wang, D., Wang, J., Luo, X., Wu, Z. & Ye, L. (2017). In Situ Preparation of Mo_2C Nanoparticles Embedded in Ketjenblack Carbon as Highly Efficient Electrocatalysts for Hydrogen Evolution. *ACS Sustainable Chem. & Engin.* 6 (1), 983–990. DOI: 10.1021/acssuschemeng.7b03317.

19. Miyake, T., Oike, M., Yoshino, S., Yatagawa, Y., Haneda, K., Kaji, H. & Nishizawa, M. (2009). Biofuel cell anode: NAD^+/glucose dehydrogenase-coimmobilized ketjenblack electrode. *Chem. Phys. Letters* 480 (1), 123–126. DOI: 10.1016/j. cplett.2009.08.075.

20. Nabae, Y., Rokubuichi, H., Mikuni, M., Kuang, Y., Hayakawa, T. & Kakimoto, M. (2013). Catalysis by Carbon Materials for the Aerobic Baeyer–Villiger Oxidation in the Presence of Aldehydes. *Acs Catalysis* 3 (2), 230–236. DOI: 10.1021/ cs3007928.

21. Tashima, D., Kishita, T., Maeno,, S. & Nagasawa, Y. (2013). Mesoporous graphitized Ketjenblack as conductive nanofiller for supercapacitors. *Mater. Letters* 110 (11), 105–107. DOI: 10.1016/j.matlet.2013.07.121.

22. Li, Y., Wang, L., He, X., Tang, B., Jin, Y. & Wang, J. (2016). Boron-doped Ketjenblack based high performances cathode for rechargeable Li–O_2 batteries. *J. Energy Chem*. 25 (1), 131–135. DOI: 10.1016/j.jechem.2015.08.011.

23. Hursan, D. & Janaky, C. (2018). Electrochemical Reduction of Carbon Dioxide on Nitrogen-Doped Carbons: Insights from Isotopic Labeling Studies. *ACS Energy Lett* 3 (3), 722–723. DOI: 10.1021/acsenergylett.8b00212.

24. Hao, Y., Lu, Z., Zhang, G., Chang, Z., Luo, L. & Sun, X. (2017). Cobalt-Embedded Nitrogen-Doped Carbon Nanotubes as High-Performance Bifunctional Oxygen Catalysts. *Energy Technol.* 5 (8), 1265–1271. DOI: 10.1002/ente.201600559.

25. Chen, C., Lu, Y., Ge, Y., Zhu, J., Jiang, H., Li, Y., Hu, Y. & Zhang, X. (2016). Synthesis of Nitrogen-Doped Electrospun Carbon Nanofibers as Anode Material for High--Performance Sodium-Ion Batteries. *Energy Technol*. 4 (11), 1440–1449. DOI: 10.1002/ente.201600205.

26. Wu, J., Yadav, R., Liu, M., Sharma, P., Tiwary, C., Ma, L., Zou, X., Zhou, X., Yakobson, B. & Lou, J. (2015). Achieving Highly Efficient, Selective, and Stable CO_2 Reduction on Nitrogen-Doped Carbon Nanotubes. Acs Nano 9 (5), 5364–5371. DOI: 10.1021/acsnano.5b01079.

27. Zhang, S., Kang, P., Ubnoske, S., Brennaman, M., Song, N., House, R. & Meyer, T. (2014). Polyethylenimine-enhanced electrocatalytic reduction of CO_2 to formate at nitrogen-doped carbon nanomaterials. *J. Amer. Chem. Soc.* 136(22), 7845–7848. DOI: 10.1021/ja5031529.

28. Xu, J., Kan, Y., Huang, R., Zhang, B., Wang, B., Wu, K. & Su, D. (2016). Revealing the origin of activity in nitrogen-doped nanocarbons towards electrocatalytic reduction of carbon dioxide. *Chem. Sus. Chem.* 9(10), 1085–1089. DOI: 10.1002/ cssc.201600202.

29. Bi, L., Ci, S., Cai, P., Li, H. & Wen, Z. (2018). One-step pyrolysis route to three dimensional nitrogen-doped porous carbon as anode materials for microbial fuel cells. *Appl. Surf. Sci.* 427. DOI: 10.1016/j.apsusc.2017.08.030.